Received: 20 September 2019 | Revised: 7 February 2020 | Accepted: 12 March 2020

DOI: 10.1002/pld3.215

ORIGINAL RESEARCH

A gravitropic stimulus alters the distribution of EHB1, a negative effector of root gravitropism in Arabidopsis

Magnus Rath[1] | Michaela Dümmer[1] | Paul Galland[1] | Christoph Forreiter[1,2]

[1]Fachbereich Biologie, Philipps-Universität Marburg, Marburg, Germany

[2]Institut für Biologie, Universität Siegen, Siegen, Germany

Correspondence
Christoph Forreiter, Institut für Biologie, Universität Siegen, Adolf-Reichwein Str. 2, D-57068 Siegen, Germany.
Email: forreiter@biologie.uni-siegen.de

Funding information
We gratefully acknowledge that this work was funded by the Deutsches Zentrum für Luft- und Raumfahrt (DLR/BMWi No. 50WB1814), granted to Christoph Forreiter.

Abstract

In Arabidopsis gravitropism is affected by two antagonistically interacting proteins, AGD12 (ADP-RIBOSYLATION FACTOR GTPase-ACTIVATING PROTEIN) and EHB1 (ENHANCED BENDING 1). While AGD12 enhances gravitropic bending, EHB1 functions as a negative element. To further characterize their cellular function, we analyzed the location of AGD12-GFP and EHB1-GFP fusion proteins in the root apex by confocal laser-scanning microscopy after gravitropic stimulation. For this purpose, a novel method of microscopic visualization was developed with the objective and root axes aligned allowing an improved and comparable discernment of the fluorescence gradient across the columella. In vertical roots, both proteins were localized symmetrically and occurred preferentially in the outer layers of the columella. After reorienting roots horizontally, EHB1-GFP accumulated in the upper cell layers of the columella, that is, opposite to the gravity vector. The gravity-induced EHB1-GFP asymmetry disappeared after reorienting the roots back into the vertical position. No such asymmetry occurred with AGD12-GFP. Our findings reveal that after a gravitropic stimulus the cellular ratio between EHB1 and AGD12 is affected differently in the upper and lower part of the root. Its impact as a significant signaling event that ultimately affects the redirection of the lateral auxin flux toward the lower site of the root is discussed.

KEYWORDS
Arabidopsis, EHB1, gravitropism

1 | INTRODUCTION

Tropic bending of plant organs is mediated by a lateral auxin gradient, which ultimately leads to a bending response toward or away from a unilateral stimulus. The gradient is established by redirection of the basal auxin flux and mediated by asymmetrically orientated cellular auxin-influx and efflux carriers of the AUX/LAX- and PIN-protein family (Adamowski & Friml, 2015; Blakeslee et al., 2007; Geisler et al., 2005). The alteration of the cellular auxin efflux is determined by a highly dynamic cellular rearrangement of plasmalemma-associated PIN-proteins, in particular PIN1, PIN2, PIN3, and PIN7, respectively. PIN-proteins continuously swap between the plasma membrane and endosomal compartments (Geldner, Friml, Stierhof, Jurgens, & Palme, 2001; Kleine-Vehn et al., 2008). A conclusion drawn from the observation was that the fungal toxin brefeldin A (BFA) drives PIN1 and PIN3 reversibly into artificial

cellular structures termed BFA compartments (Geldner et al., 2001; Naramoto, 2017). BFA inhibits vesicular traffic by affecting ARF-GEF proteins (ADP-ribosylation factor guanine-nucleotide exchange factors), required for GTP/GDP exchange of their target proteins termed ARFs (ADP-ribosylation factors). ARFs represent a group of small GTPases, which play a prominent role in plant development by establishing endosomal vesicle trafficking of various molecules (Hwang & Robinson, 2009; Robinson et al., 2018). ARF-GEF action enables ARF cycling and thus PIN-redirection from an endosomal compartment to the polar domain at the plasma membrane. If ARF-GEF is inhibited by BFA treatment, PIN-proteins accumulate in the emerging BFA compartments. This has been previously shown for GNOM, an Arabidopsis ARF-GEF protein. *gnom*-mutants reveal severe defects in development because coordinated cell polarities were not established correctly (Richter et al., 2010). *gnom*-mutants are also impaired in gravitropism by loss of the correct cellular PIN1 localization (Geldner et al., 2003; Steinmann et al., 1999). Previously, it could be shown that GNOM acts directly at the Golgi apparatus (Naramoto et al., 2014), indicating that GNOM may be more indirectly affecting the functionality of trans-Golgi/early endosome traffic. Nevertheless, GNOM affects ultimately the basal targeting of PIN proteins and by this cellular auxin efflux, which affects gravitropism negatively (Kleine-Vehn et al., 2008).

However, ARF-mediated membrane traffic requires not only GTP exchange but also GTP hydrolysis mediated by a corresponding AFR-GAP element. Thus, it is likely that not only ARF-GEFs such as GNOM but also ARF-GAPs (ARF GTPase-activating protein) play an important role in gravitropic bending. ARF-GAPs belong to a small protein family, which share a common ARF-GAP motif, enabling the protein to interact with ARFs. One of them, termed ZAC (zinc-finger/ARF-GAP/C2) or as in Arabidopsis AGD12 (ADP-ribosylation factor GTPase-activating protein) mediates GTP hydrolysis by ARF1 or ARF3 in vitro (Jensen et al., 2000)and affects, as anticipated, gravitropism. We have previously shown that gravity- and light-induced root bending is positively affected by AGD12 (Dümmer et al., 2016; Michalski, Dümmer, Galland, & Forreiter, 2017). Beside a canonical ARF-GAP domain required for GTP hydrolysis AGD12 contains also a C2, or alternatively CaLB (Calcium lipid binding) domain enabling the protein to bind phospholipids, phosphoinositide, and proteins in a calcium-dependent manner (Nalefski et al., 2001). Given the prominent role small G-proteins play in auxin-mediated tropisms, we were interested to understand, whether or not EHB1, which is an early effector in light- and gravity-mediated signaling (Knauer, Dummer, Landgraf, & Forreiter, 2011), could also operate via small G-protein interaction. In contrast to AGD12, EHB1 acts as a negative regulator in phototropism and gravitropism. EHB1 is a rather small protein, consisting only of a C2 domain that is homologous to the C-terminal region of ADG12, while an ARF-GAP motif is missing. Of all known members belonging to the ARF-GAP protein family only AGD11, 12, and 13 possess a comparable C2 motif similar to that of EHB1 (Vernoud, Horton, Yang, & Nielsen, 2003). Although not all C2 domain-containing proteins need Ca^{2+}-ions for lipid binding, all of the so far described C2 domain-containing proteins involved in GAP regulation do depend on calcium (Sot, Behrmann, Raunser, & Wittinghofer, 2013). Because of the intriguing homology of the C-terminal parts of AGD12 and EHB1 and their antagonistic interaction in phototropic and gravitropic bending, we hypothesize that AGD12 might act as a default element for ARF-driven GTP hydrolysis ensuring normal endosomal traffic, while EHB1 acts as an inhibitory element by binding to ARF counteracting this way ARF-GAP activity. Recently, it was shown that Ca^{2+}-bound EHB1 attaches to the membrane and inhibits iron uptake by interacting with the iron-regulated transporter IRT1 in Arabidopsis (Khan et al., 2019).

To further characterize the localization of both proteins after gravitropic stimulation, we developed a special confocal laser scanning microscopy technique called end-on visualization (see below) to monitor EHB1-GFP and AGD12-GFP expression in roots tips. We describe in this work that in vertical roots EHB1-GFP and AGD12-GFP were differently distributed within the calyptra. In cross-sections of root tips, a differential fluorescence pattern could be observed for both proteins, if plants were vertically grown. The signal fades in more basipetal regions before entering the transition zone. Additionally, we could show a gravity-dependent effect on the tissue distribution of EHB1 in gravitational stimulated root cap tissue. Our data provide evidence that the distribution EHB1, but not of AGD12, is affected after a gravitropic stimulus.

2 | MATERIAL AND METHODS

2.1 | Plant material and growth conditions

All experiments were performed with lines of Arabidopsis thaliana (L.) Heynh., ecotype Columbia, containing either EHB1-GFP or AGD12-GFP, expressed under control of a 35S-CaMV promoter, which have been previously described (Dümmer et al., 2016). To analyze the native EHB1 expression, an Arabidopsis line was generated, which contained a genomic fragment of 629 nucleotides upstream of the EHB1 open reading frame fused to a EGFP-reporter protein. The sequence was obtained by genomic PCR using genome derived sequence-specific primer (5′-primer:CACCGATGCAGAA ATGTTAAAACAG/ 3′-primer: CTTGCTTCTGAGCTTTGAAGAGAAAG). The upstream primer was located within the 3'-UTR of the proximate upstream open reading frame (AT1G70790). The fragment was blunt ligated into a gateway pENTR/D-topo entry vector and transformed into *E. coli* TOP10 for further propagation according to the manufactures protocol (Invitrogen/Thermo Fisher). The sequence was subsequently introduced into a binary destination vector pKGWFS7 providing an EGFP open reading frame fused to a 35S-CaMV-terminator within the Ti-plasmid left and right border sequence (Karimi, Inze, & Depicker, 2002). The resulting construct was verified by sequence analysis and transformed into an *Agrobacterium tumefaciens* GV3101 stain. The stain was subsequently used to transform *A. thaliana* Col-0. (wild type) via floral dip transformation (Clough & Bent, 1998). Successfully, transformed seedlings were identified by genomic PCR and RT-PCR. GFP mRNA expressing seedlings were further backcrossed to obtain homozygous lines. Seedlings containing a

35S-CaMV:GFP construct used as a fluorescence controls were obtained from Thomas Schmülling (Werner et al., 2003). Seeds were sterilized using 95% (v/v) ethanol and 5% (v/v) sodium hypochlorite and then sown on half-strength Murashige and Skoog salts medium (MS-medium; Sigma) containing 25 mM MES sucrose. Plates (rectangular, 100 × 100 mm, 20 mm height) with seeds were maintained for 2 days in darkness at 5°C and subsequently placed for 7 hr under white fluorescent overhead light (10 µmol m^{-2} s^{-1}) to induce germination. After induction of germination, plates were stored for three days in the dark at 21.5°C in a vertical position. Doing so a symmetrically distribution of the analyzed GFP proteins in the root cap could be ensured. Following this pre-treatment an initial microscopic scan was made (t = 0), which served as a starting point. A subsequent gravitropic stimulation was administered by tilting the object holder with the seedling (Figures 1 and 2) for varying durations as indicated in the result part.

2.2 | Root pre-treatment for confocal microscopy

To prevent any phototrophic light stimulation of the roots, all preparations were done under red safelight (680 nm). Deploying confocal

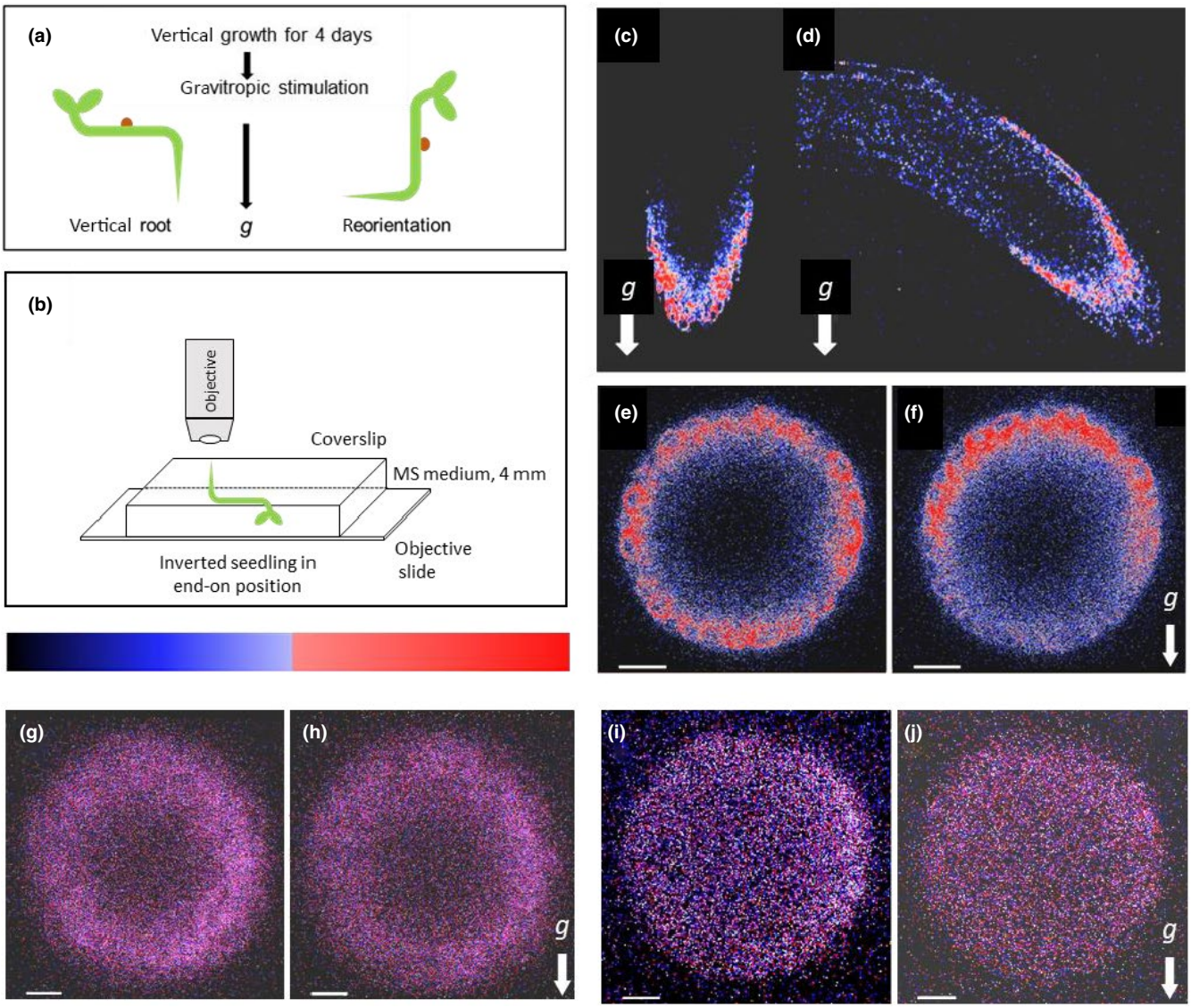

FIGURE 1 Fluorescence micrographs of vertical and 90° tilted roots expressing EHB1-GFP, AGD12-GFP, and GFP under control of a 35S-CaMV promoter, respectively. (a) Experimental setup for a gravitropic stimulus. Seedlings were grown vertically for 68 hr in the dark, presented in C, E, G, and I, respectively. (b) After that seedlings were tilted 90° and left for additional 101 min in the dark shown in D, F, H, and J. (c,d) Images of EHB1-GFP fluorescence in which the axis of the microscope objective is perpendicular to the root axis. (e,f) Same seedlings analyzed from the root tip ("end on"). (e) Vertically grown roots revealed a symmetric distribution of EHB1-GFP. (f) In reoriented roots, EHB1-GFP fluorescence got asymmetrically distributed or polarized with enhanced fluorescence at the top and reduced fluorescence at the bottom. AGD12-GFP (g,h) and GFP alone (i,j) expressing roots do not show any gravitropically induced redistribution. Images were taken 80 µm above the root tip. *g* = direction of the gravitational acceleration. Scale bar = 15 µm. The relative fluorescence in this and the following figures were quantified and displayed as heat map, were high fluorescence is shown in red and moderate expression in blue

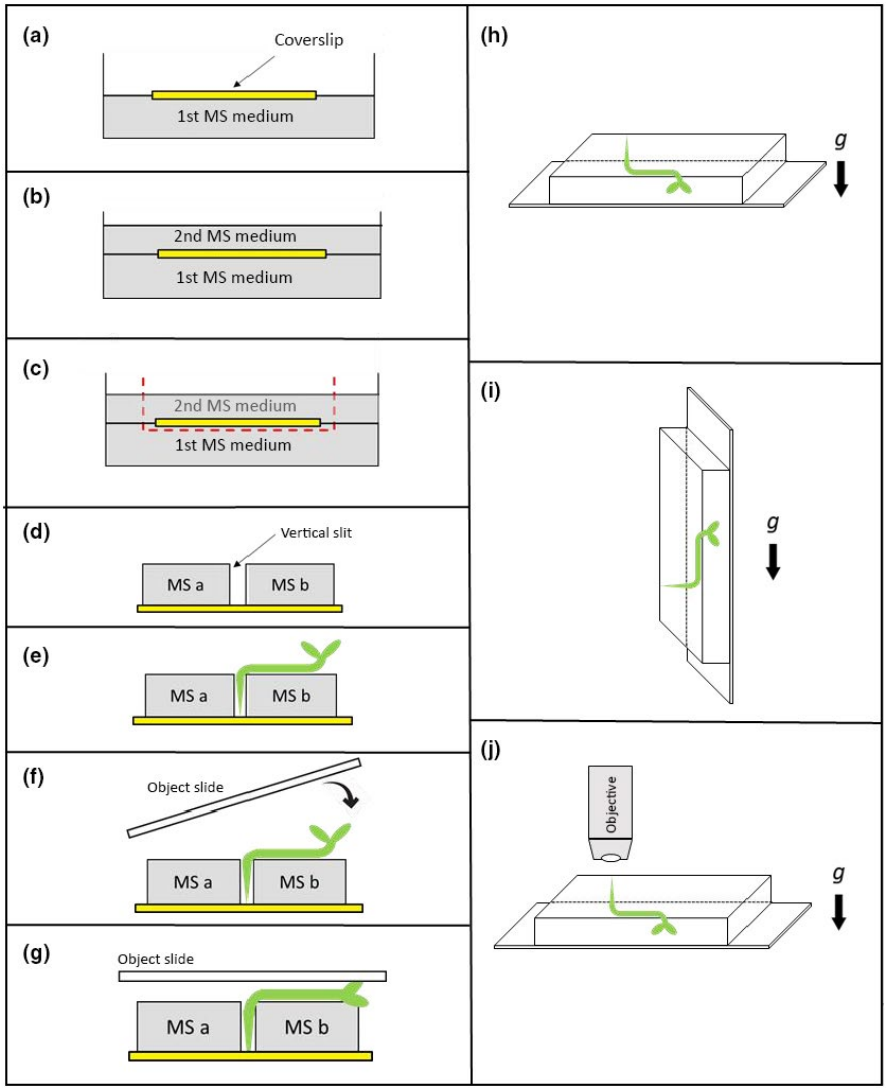

FIGURE 2 Seedling preparation for end on analysis. (a) At first a sterile coverslip (yellow) was placed on solid MS-agar medium. (b) A 2nd layer of MS-agar medium was poured on top of the first layer, covering the applied coverslip. (c) Parts of the top agar (including the coverslip) were removed. (d) The cut-out block on top of the coverslip was separated in two agar blocks (MS a & MS b) forming a small slit. (e) Seedlings were transferred with a tweezer onto the agar with the root tip fixed between the two blocks. (f,g) Finally, an object slide was placed gently on top of the seedling. (h) After preparation of the seedling (as presented in a-g), roots were allowed to grow vertically toward the coverslip. (i) For application of a gravitropic stimulus, a 90° turn of the objective slide for 1–4 hr was applied. (j) Position of the specimen and objective lens during confocal analysis

microscopy in the common configuration (objective perpendicular to the root axis), it was also possible to determine an asymmetry of GFP-EHB1 fluorescence intensities. However, when reconstructing the optical X-Z-plane, scattering along the Z-axis (top/bottom) could be observed, which would become unequal in a way that fluorescence intensities of GFP-EHB1 at top and bottom would be differently affected. The net result is an artifactual change of the real spatial asymmetry of GFP-EHB1 in the root cross-section, which would be hard to correct (e.g., by calculating or measuring scatter increases along the *Z*-axis).

To overcome this an alternative way to analyze the distribution of EHB1 and AGD12 in root tissue was deployed and outlined in Figure 2. After preparing a suitable coverslip (Figure 2a-c) seedlings were carefully removed with a tweezer from a vertically orientated agar plate and transferred to two blocks of MS-medium (Figure 2d,e) such that the rootlets came to rest vertically inside the slit between the two MS-blocks, while the hypocotyls were laid horizontally on the surface of the MS-medium. In the next two steps, an objective slide was gently placed on the seedling (Figure 2f,g), which was then adapted for 3 hr to the new environment with either vertical or horizontal roots, respectively (Figure 2h,i). For microscopy, the entire assembly containing coverslip, MS-agar blocks, and seedling was carefully turned upside down and mounted onto a glass slide (Figure 2j). Subsequently, a drop of immersion medium (water) was placed on top of the slip. Alternatively, plates and seedlings were placed horizontally for one day. Thereby roots do now grow into the MS-phytagel toward the coverslip resulting in a 90° hook-like structure of the root. Usually, after 24 hr a few root caps suitable for further analysis are about 0.5–1 mm away from the coverslip. This turned out to be a good position for microscopic analyzes using water immersion objectives with a 20-fold or 40-fold magnification, respectively. Prior microscopy the whole assembly was excised, carefully turned upside down and placed on a glass slide with a drop of immersion medium placed on top (Figure 1). Etiolated Arabidopsis seedlings were viewed in a TCS SP2 confocal unit (Leica) mounted onto a Leica DMRB upright microscope. Unless otherwise stated, confocal fluorescence optical sections were taken with a HCX PL APO × 40/1.25–0.75 Oil CS (Leica) objective or alternatively with a HCX APOL40×/0.8 W water-immersion objective with twofold to eightfold line average at a resolution of 1,024 × 1,024 pixel and a z-resolution of 1–5 µm.

GFP constructs were excited with the 488 lines of an Argon laser (65 mW). Reference images were taken with differential interference contrast optics. For each root, the photomultiplier gain was kept in the linear range between scans to allow a comparison of fluorescence intensities. The look-up table "glow" was chosen for color presentation of scans, indicating increase of fluorescence intensity by pixel color ranging blue (weak signal) to red (strong signal). Image stacks are presented as maximum projection.

2.3 | Inhibitor application

Prior gravitropic stimulation by reorientation (90° tilt) either 10 µg/ml cytochalasin-D, 100 µM cycloheximide, 10 µM brefeldin A, 50 µM/N-naphthylphthalamic acid (NPA), or 1.0 µM indole acetic acid were applied, respectively. To allow a homogeneous inhibitor distribution within the tissue, seedlings were carefully removed from the MS medium and placed exactly in the same position as before (i.e., parallel to *g*) between two inhibitor-containing phytagel blocks, as shown in Figure 2. After 1 hr incubation with the indicated inhibitors, the vertical root caps were scanned to define the default fluorescence distribution. After gravitropic stimulation and incubation for at least 60 min roots were scanned and analyzed for changes in their GFP-fluorescence.

2.4 | Gravitropism experiments

To correlate the distribution of EHB1 inside the root tip with the resulting bending angle after gravitropic stimulation, 3-day-old etiolated seedlings were placed on MS phytagel containing either 10 µM brefeldin A, 100 µM cycloheximide, 10 µg/ml cytochalasin D, 50 µM/N-naphthylphthalamic acid (NPA) or 1 and 50 µM auxin, respectively. After that, seedlings were horizontally reoriented and kept for another 20 hr in the dark at 20°C. Subsequently, the resulting bending angles of the roots were determined. Mean values and standard errors were calculated for 30–40 specimens.

2.5 | Quantification of the temporal EHB1-GFP fluorescence asymmetry after a gravitropic stimulus

Roots were prepared as indicated above and scanned directly before gravitational stimulation (t = 0). After reorientation (90° tilt), root caps were scanned repeatedly for the indicated time frame. Scan images of each time point were adjusted to an identical position toward the z-axis, and the mean grayscale light value in a defined elliptical section (region of interest; ROI) was measured and quantified by using the ImageJ software (ImageJ, Vers. 1.48). Two distinct regions of interest (ROI) were defined: ROI 1 was set at the upper side of the root, while ROI 2 was set at the lower side of the root cap cross-section. Subsequently, all obtained data were normalized to t = 0 and afterward the ratio of ROI 1 and ROI 2 was calculated. The ratio was set 0%, while the ratio of the last scan was set as 100%.

3 | RESULTS

3.1 | Seedling preparation for end-on visualization

In our previous work, we presented evidence that EHB1 and AGD12 are localized preferentially in the columella of the root, specifically its lateral part (Dümmer et al., 2016). In those microscopic studies, we employed traditional methods of sample preparation in that the roots laid flat on the objective slide and were thus oriented perpendicularly to the axis of the microscope objective. This way we could obtain longitudinal optical sections of the root that are suitable to detect, though not perfectly well, a gravity-induced asymmetry of EHB1-GFP fusion protein (Figure 1c,d). To obtain a better spatial resolution for documenting the gravity-induced asymmetry of EHB1-GFP across the root cap, we abandoned the traditional way of microscopic sample orientation and adopted a different procedure, in which the axis of the root and the microscope objective are aligned such that the objective lens and the root apex are facing each other vis-à-vis (Figure 1b). We refer to this mode of sample orientation and subsequent microscopy as "end-on visualization" (Figure 1e,f). The novel method allows a determination of the fluorescence-intensity ratios (top/bottom) across the root tip with a minimum of optical artifacts. Usually, the configuration commonly employed in confocal microscopy achieves a superior optical resolution in optical layers close to the objective, while the top/bottom fluorescence-intensity differences are more prone to scatter artifacts, particularly, when one has to cope with unusually large optical depths of up to 120 µm as in our experiments (see Figure 3). The advantage of end-on visualization in this particular case is that despite the usual scatter associated with confocal microscopy, the upper and the lower zones of interest (ROIs) possess, because of identical optical distances from the root apex (e.g., Figures 1 and 3), the same scatter-generated fluorescence blurring and loss. Thus, end-on configuration is optimized for quantifying fluorescence-intensity differences between bottom and top in root cross-section at cost of diminished optical resolution. However, sample preparation for end-on visualization was elaborate and required a sequence of manipulations of seedlings, which have been described in detail in the method part.

3.2 | Expression patterns of EHB1-GFP and AGD12-GFP in vertical and horizontal root caps

The effects of AGD12 and EHB1 on root gravitropism (Dümmer et al., 2016) prompted us first to analyze the overall GFP fluorescence of AGD12-GFP and EHB1-GFP seedlings in roots. Transgenic plants expressing constitutively either an EHB1-GFP or AGD12-GFP fusion construct under control of a 35S-CaMV promoter were analyzed for their localization within the root cap after a given gravitational stimulus. Three-day-old vertical seedlings were horizontally reoriented as shown in Figure 1a and analyzed by confocal laser scanning microscopy immediately before tilting. After keeping them for 101 min in a

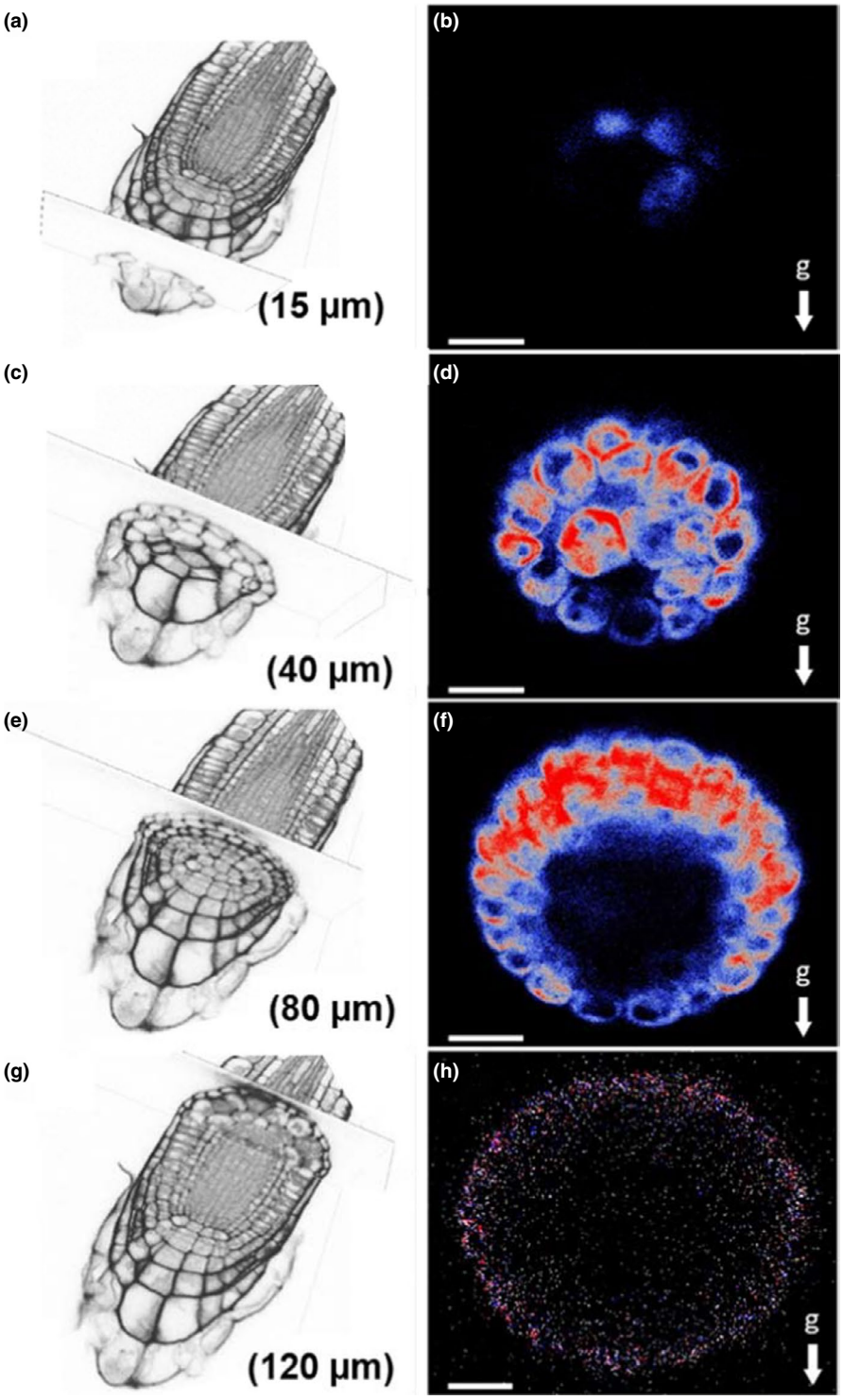

FIGURE 3 EHB1-GFP expression in roots that were kept horizontally for 48 min prior to microscopy. Root caps were either scanned at 15 µm (a,b), 40 µm (c,d), 80 µm (e,f), and 120 µm (g,h) depth, respectively. Left: section overview obtained from phase-contrast microscopy. Right: confocal images of the EHB1-GFP asymmetry in dependence from the distance to the root tip (end-on visualization). EHB1 is located preferentially in the peripheral layers of the root cap between 40 and 80 µm, in which also the asymmetry is observed after gravistimulation. EHB1-GFP is also found at 40 µm in the central statocytes of the columella (d). *g* = gravitational acceleration. Scale bar = 15 µm

horizontal position, images were taken 80 µm basipetally from the tip. Confocal fluorescence analysis with end-on visualization revealed a circular and symmetric expression of EHB1-GFP and AGD12-GFP prior tilting (Figure 1e,g), while GFP alone was more or less arbitrarily distributed across the root tissue (Figure 1i and Figure S1). After reorienting seedlings horizontally, the fluorescence pattern of EHB1-GFP altered markedly and shifted toward the upper part of the root cap (Figure 1d,f, Data S3), while below the axis of the horizontally orientated root the fluorescence signal faded. In contrast to EHB1-GFP the overall distribution of AGD12-GFP and GFP alone, which served as a control, was not affected (Figure 1h,j, Figure S2).

3.3 | EHB1 is only weakly expressed in root tip tissue

The above describe EHB1 overexpressing line was originally generated to analyze the cellular distribution of EHB1 and AGD12

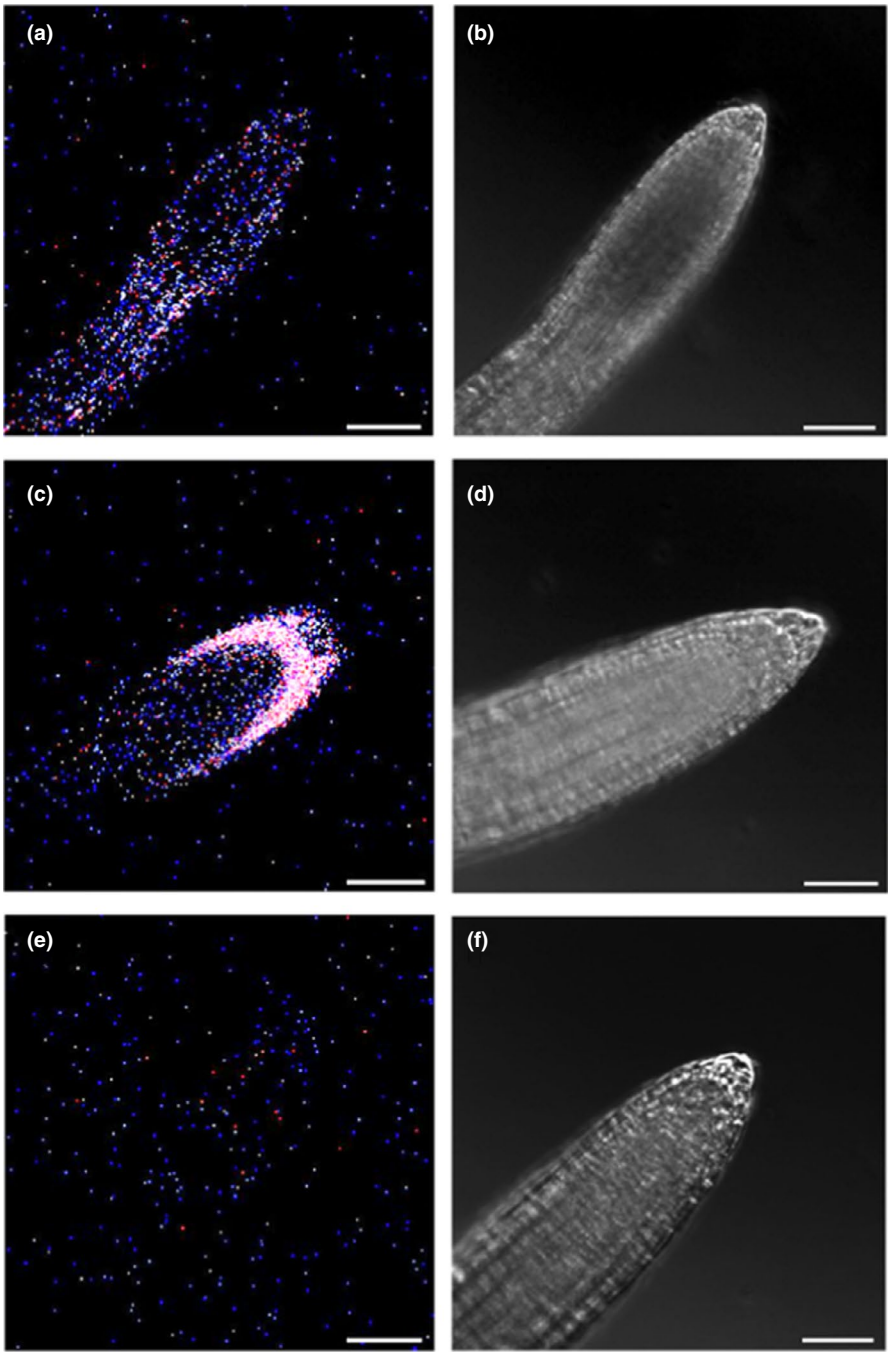

FIGURE 4 Tissue expression of a GFP-reporter protein expressed under control of a native EHB1 promoter. (a) GFP-fluorescence of GFP expressed under control of a native EHB1 promoter (see methods for details). (c) For comparison, GFP fluorescence of EHB1-GFP expressed under control of a 35S-CaMV promoter and (e) autofluorescence of non-transformed Col 0 were shown. (b,d,f) Corresponding phase-contrast images. The detection window of the confocal microscope was set to 509 nm (±5 nm) to comprise the maximum peak of GFP fluorescence. Images of the native EHB1-promoter construct revealed only a very low fluorescence at 509 nm compared with the strong and distinct GFP-fluorescence of the 35S-promoter construct. Although the native EHB1 promoter showed significantly more fluorescence at 509 nm than the wild-type strain, confocal microscopic methods could not clearly distinguish GFP and residual autofluorescence in the native EHB1 promoter construct and were therefore not used for further analysis

presented earlier (Dümmer et al., 2016). The observation that EHB1, in contrast to AGD12 and GFP alone, got asymmetrically distributed in overexpressing seedlings after a gravitropic stimulus, prompted us to analyze the spatial and temporal expression of EHB1 using a reporter line expressing EHB1-GFP under control of a native EHB1-promoter. However, the resulting GFP fluorescence in gravitropically stimulated roots was only barely visible (Figure 4). The result was further hampered by the fact that tissue autofluorescence made it almost impossible to distinguish a GFP signal from noise. Only a wavelength-dependent differential calculation revealed a small amount of GFP-related fluorescence, indicating the presence of the protein. Unfortunately, this signal was too faint to provide reliable data for subsequent confocal analysis.

3.4 | EHB1-GFP distribution in different root cap zones after a gravistimulus

Further experiments were thus performed using the EHB1-GFP expressing lines driven by the above described 35S-CaMV promoter. Root cross-sections were investigated by scanning at different focal depths of the cap (Figure 3 and Data S3). It became apparent that the asymmetric EHB1-GFP distribution in gravitropically stimulated roots was differently pronounced in different physiological zones of the root cap. In the cap cells of the calyptra, the upper cells revealed a considerably stronger EHB1-GFP fluorescence than the lower ones. This effect was gradually more enhanced toward the meristematic zone. Beyond 120 µm the signal faded (Figures 1c and 3h).

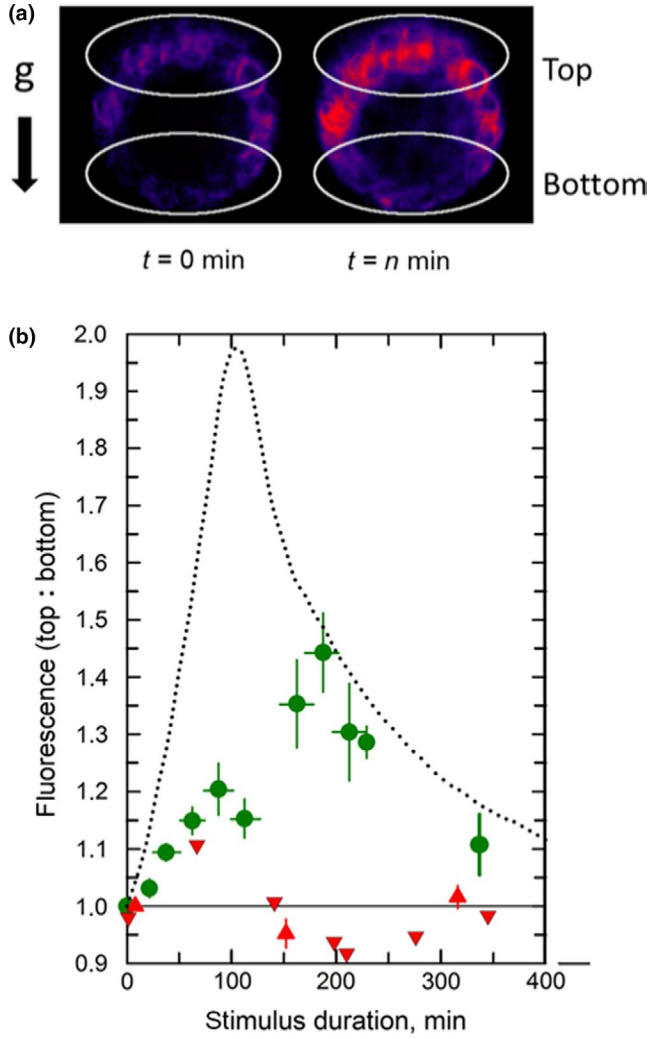

FIGURE 5 Kinetics for the development of the EHB1-GFP fluorescence asymmetry (F_{top} vs. F_{bottom}) in gravitropically stimulated roots. (a) To quantify the fluorescence intensity, two regions of interest (white circles) were defined for which the fluorescence intensities were determined. (b) Prior reorientation (t = 0) end-on images were taken 80 µm from the root apex of a vertically grown root and compared with an end-on images obtained from gravitropic stimulated (horizontally orientated) roots. The ratio of both regions was plotted over time (green dots). Black-dotted line: kinetics for the redistribution of endogenous IAA (redrawn from Band *et al*., 2012). Red upward-pointing triangles: roots were treated omnilateral for 10 min prior t = 0 with 1 µM IAA, which remained present during stimulus durations. Red downward-pointing triangles: Roots were treated for 10 min prior t = 0 with 10 µM NPA. Vertical errors bars: SE of 12–22 specimens. Horizontal error bars indicate the time intervals (SE) from which the data were binned

3.5 | Time course of EHB1-GFP redistribution in horizontally orientated roots

Next, the temporal dynamics of the EHB1 fluorescence redistribution within the elongation zone has been analyzed in a more quantitative approach (Figure 5). For this purpose, two regions of interest (ROI) were defined, for which fluorescence intensities were

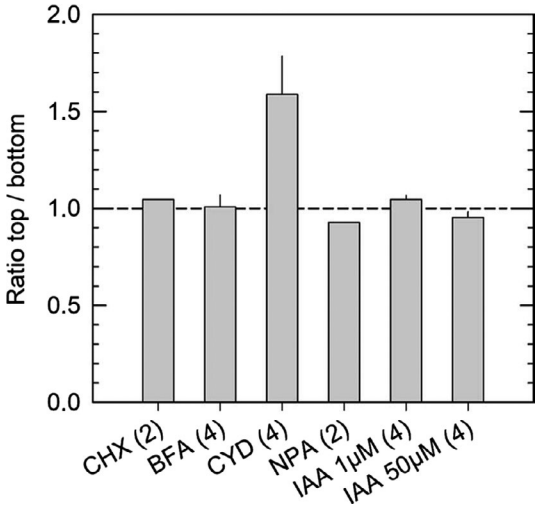

FIGURE 6 Ratio of the fluorescence intensities of EHB1-GFP in horizontally placed root tips that had been treated with the inhibitors shown in Figure 8. The two regions of interest, that is, ROI 1 at the top and ROI 2 at the bottom of the roots were as defined in Figure 5. Prior microscopy roots were unilaterally exposed for at least 1 hr to the various inhibitors (see Figures 8 and 9). Numbers of analyzed roots are given below the columns. BFA, brefeldin A; CHX, cycloheximide; CYD, cytochalasin D; IAA, Indole acetic acid; NPA, N-1-naphthylphthalamic acid. Mean values are given. Error bars, if any, indicate *SE*

measured (Figure 5a). The fluorescence intensity in both regions was compared and provided a ratio between F_{top}/F_{bottom}. The resulting kinetics is presented in Figure 5b. The extrapolated latency for a detectable increase of the ratio value (i.e., increase of the EHB1-GFP fluorescence at the upper side of the horizontal root) was approximately 5–10 min. The ratio value reached a maximum after 3 hr. Once established in horizontal roots, the asymmetry remained stable. Notably, in presence of 1 mM auxin as well as 10 µM NPA and in line with the observation presented in Figure 6, no asymmetrically distribution could be observed (Figure 5b, upward- and downward-pointing red triangles).

3.6 | EHB1-GFP distribution is dependent on the orientation of the root

Considering that changes of the EHB1 fluorescence ratio during gravitropic stimulation represent an essential element of the signal transduction chain, the ratio should decrease again after reorienting horizontal roots vertically. This assumption was fully supported by data shown in Figure 7, which displayed a kinetic for the diminution of the fluorescence asymmetry in roots that were reoriented again vertically. It became apparent that the fluorescence ratio resumed to values of the initially omnilateral symmetric fluorescence after approximately 5–6 hr (Figure 7e). It is noteworthy that the maximum asymmetry observed after approximately 3 hr was balanced again after 5 hr in vertical position. The kinetics could be substantially accelerated, if exogenous auxin was

applied 20 min before the roots were brought back into a vertical position (Figure 7e, red symbols).

3.7 | The polarization of EHB1-GFP is affected by cycloheximide, brefeldin A, and NPA, but not by cytochalasin D

To better understand the mechanisms that possibly participate in the redistribution of EHB1-GFP after a gravitropic stimulus, individual roots were treated with inhibitors affecting different cellular processes, which might be involved in the accumulation of EHB1-GFP on the upper side of the root. During vertical growth, roots were incubated for 1 hr with different inhibitors. Seedlings were analyzed by confocal end-on microscopy, tilted 90° for 60 min and subsequently analyzed a second time (Figure 8). To confirm these results several seedlings were analyzed and the EHB1 fluorescence between top and bottom was quantified and compared (Figure 6). First, we inhibited protein synthesis by applying cycloheximide. As shown in Figure 8a,b cycloheximide effectively blocked any redistribution of EHB1-GFP, and in addition, disabled root bending after reorientation (Figure 9). Second, we took advantage of the fact that artificial endosomal vesicles were formed upon treatment with the fungal toxin brefeldin A (Pelham, 1991). Since EHB1 and AGD12 could be found in BFA compartments (Dümmer et al., 2016), we were interested to know, if trapping EHB1 in BFA compartments had an impact on EHB1-GFP fluorescence and bending after reorientation. Indeed, as shown in Figures 6 and 8c,d, BFA subdued EHB1-GFP redistribution to the upper side of the root and also reduced gravitropic bending by 80% (Figure 9). A similar effect on EHB1-GFP distribution and bending could be observed, if NPA was applied. NPA inhibits the auxin flux by affecting PIN protein redistribution, probably by distorting vesicular traffic by interacting with GNOM, an ARF-GEF protein (Geldner et al., 2003). As expected and already frequently shown, gravitropic bending was entirely abolished by NPA treatment (Figure 9), an observation that correlated with an inhibition of EHB1 relocation (Figures 6 and 8e,f). Although root bending was significantly reduced after treatment with cytochalasin D (Figure 9), the EHB1-GFP relocation remained unaffected (Figures 6 and 8g,h), indicating that the cytoskeleton plays only a marginal role in the EHB1 dynamics and that symplastic transport can be ruled out as a transport system for the relocation of EHB1. Comparable to NPA, exogenous auxin abolished the asymmetric EHB1 fluorescence gradient (Figures 6 and 8i,j). This observation was in line with the effect presented in Figures 5 and 7. Additionally, and in comparison with the other inhibitors, it could be observed that after auxin treatment the overall EHB1-GFP fluorescence intensity was reduced in the investigated tissue, but varied considerably among individual roots.

4 | DISCUSSION

We have previously shown that AGD12 and EHB1 act antagonistically in roots after a phototropic or gravitropic stimulus (Dümmer

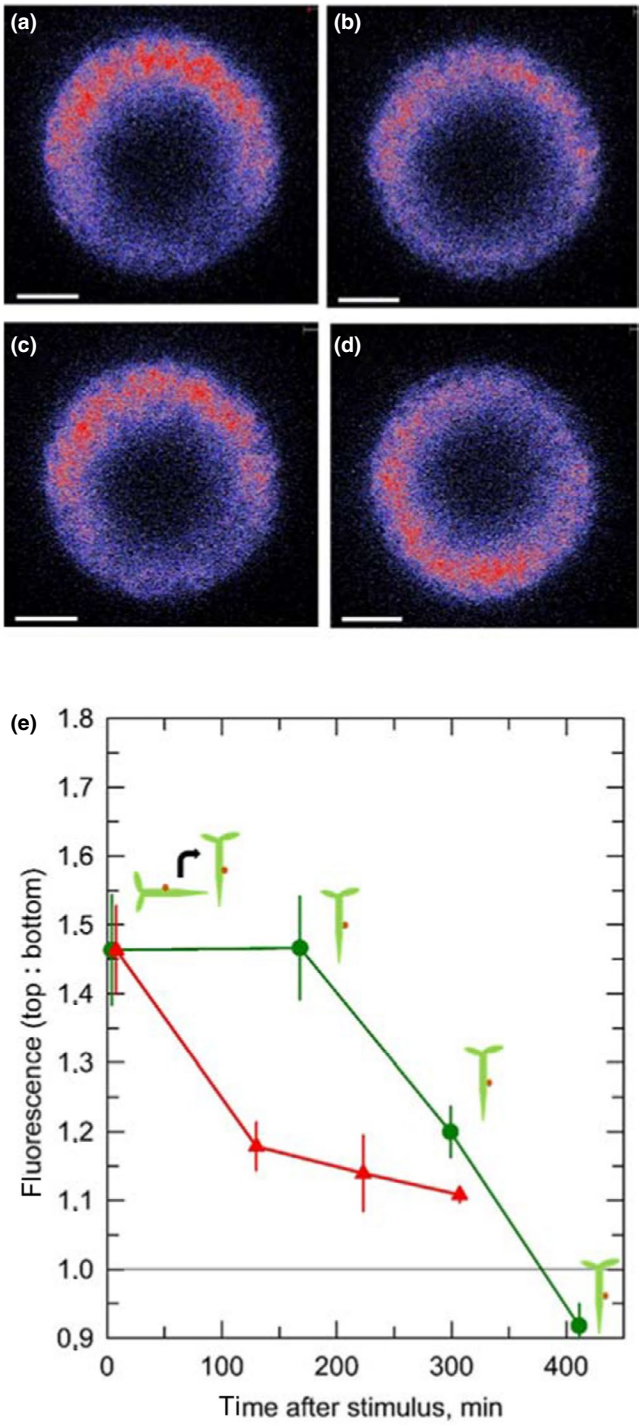

FIGURE 7 Roots which had been kept horizontally for 3 hr were reoriented vertically again and maintained vertically for the indicated durations. (a) Immediately after redirecting the roots in a vertical position an end-on image was taken 80 µm from the root apex. (b-d) Same seedling after the indicated time of vertically growth. (e) For quantification, two regions of interest (F_{top} and F_{bottom}) were defined (see Figure 5) and the fluorescence ratio was determined (green dots). If auxin was applied 20 min before the seedlings were tilted back into a vertical position (red triangles), the equilibrium was reached much quicker. Vertical errors bars: *SE* of 4 independent determinations of fluorescence intensities

et al., 2016; Michalski et al., 2017). To better understand the cellular basis for this antagonistic operating system, we analyzed in detail the spatial distribution of EHB1-GFP and AGD12-GFP in roots. We were able to show that although under control of a 35S-CaMV promoter, both proteins were in contrast to GFP alone, differentially expressed in vertical roots in such a way that EHB1-GFP and AGD12-GFP were ring-like distributed within the root tip (Figure 1e,g; (Dümmer et al., 2016). This observation points to an active downregulation of AGD12 and EHB1 in areas of the root were an expression of one of the proteins may be unfavorable. However, a positioning effect induced by the t-DNA insertion cannot be ruled out, since only one transgenic line was analyzed so far. After a gravitropic stimulus, EHB1 was actively redistributed in the root tip. After reorienting vertically roots horizontally, EHB1 accumulated in the upper peripheral cell layers of the root cap. In this area, the ratio between EHB1 and AGD12 got thus shifted in favor of EHB1. Because EHB1 and AGD12 operate antagonistically (Dümmer et al., 2016), the relative excess of EHB1 in the upper side should lead to a reduced activity of AGD12, which functions as an ARF-GAP protein. We propose that the reduced ARF-GAP activity leads in turn to a reduced ARF-mediated vesicle trafficking resulting in disabling PIN protein traffic and thus a diminished auxin flux in the upper side (Figure 10). In vertically grown roots, in which EHB1 and AGD12 are distributed symmetrically, auxin is transported downwards within the vascular cylinder, a process facilitated by PIN1. It has previously been shown that as soon as auxin reaches the area of the columella, the hormone gets radially distributed by a symmetrically lateral distribution of PIN3 and PIN7 and later ascends in the endodermal and cortex tissue of the root mediated by PIN2 (Petrasek & Friml, 2009). If ARF dephosphorylation is negatively affected in the upper part of the root, this might block the auxin flux to the upper epidermis layer. Only few cells would be required to block an upward auxin flux, an assumption, which is supported by the observation that in root tissue EHB1-GFP under control of a native promoter is only weakly expressed (Figure 4). Thus, only a small amount of EHB1 needs to be relocated and the marked fluorescence effect which could be observed here reflects the massive production

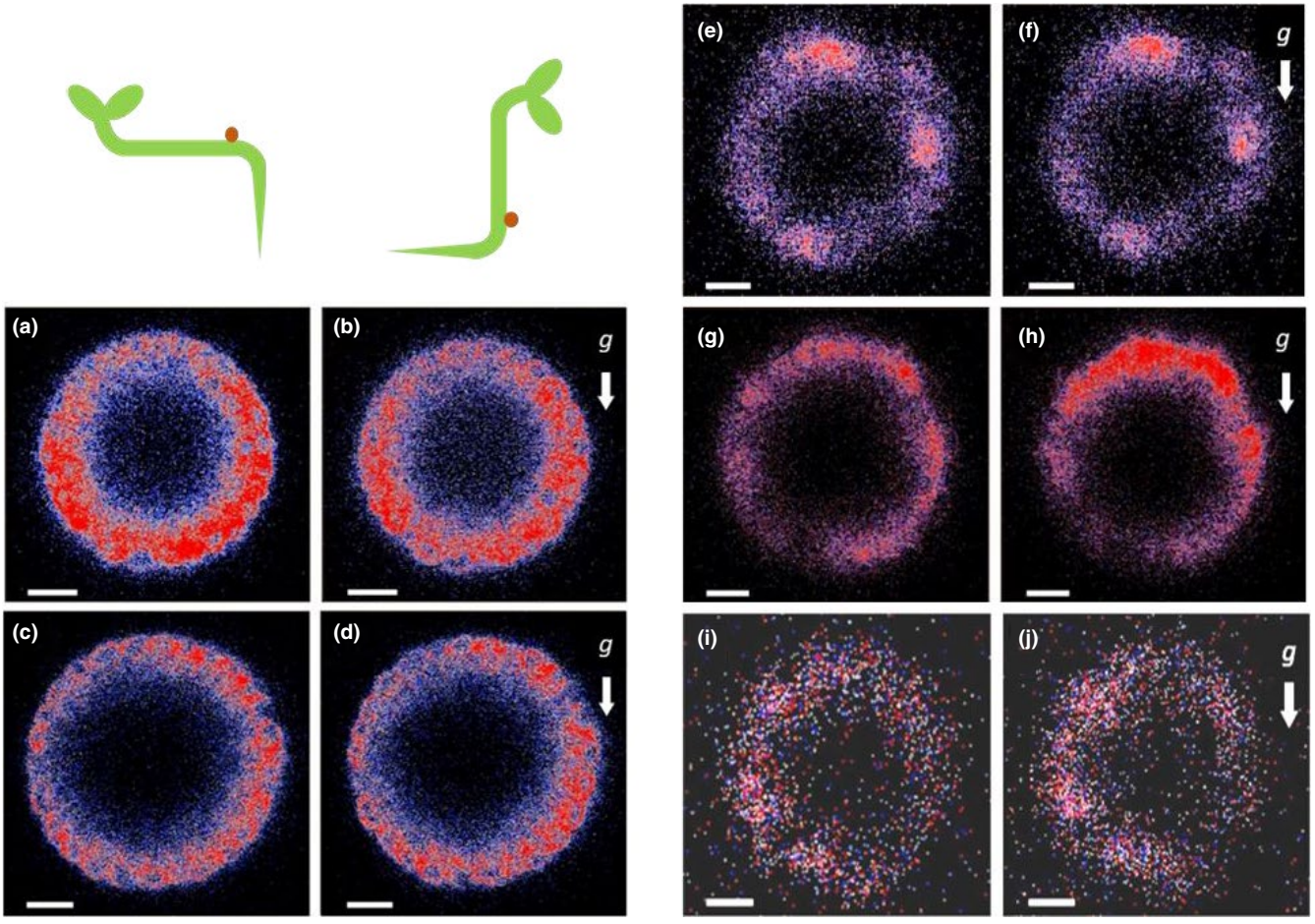

FIGURE 8 Effect of various inhibitors on the differential fluorescence signals ofEHB1-GFP in vertical and horizontal root caps. Optical cross-sections obtained from end-on visualization were taken at a depth of 80 µm. Scans of vertical roots treated with the inhibitors were taken (a, c, e, g, and i, respectively). Subsequently, roots were reoriented and kept for at least 60 min horizontally (b, d, f, h, j) before they were analyzed a second time. Prior microscopy vertical roots were unilaterally exposed for 1 hr to various inhibitors. (a,b) cycloheximide (CHX, 100 µM); (c,d) brefeldin A, (BFA, 10 µM), (e,f) N-1-naphthylphthalamic acid (NPA; 50 µM); (g,h) cytochalasin D (CYD, 10 µg/ml); (i,j) Indole acetic acid (IAA, 1 µM). *g* = gravitational acceleration. Scale bar = 15 µm

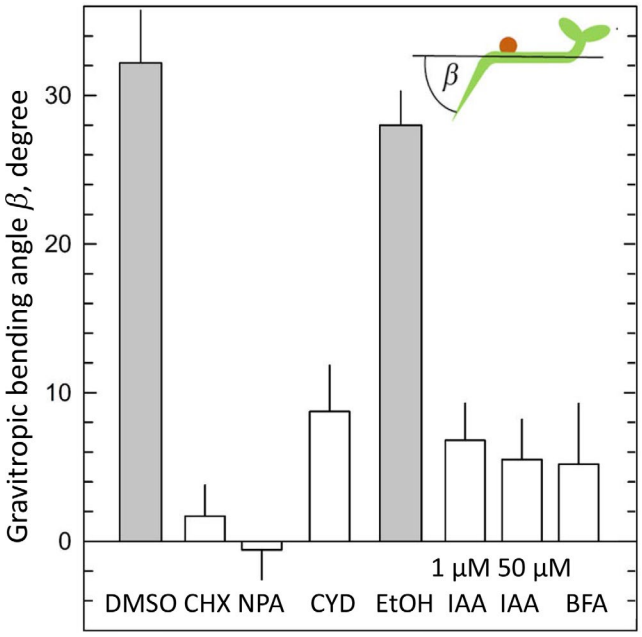

FIGURE 9 The effect of various inhibitors on the gravitropic bending of roots of the EHB1-GFP overexpressing expressing strain (Dümmer et al., 2016). Vertically raised seedlings were tilted 90°, and the gravitropic bending angles were determined after 20 hr in darkness. The seedlings were treated with the same inhibitor concentration that also affected the distribution of EHB1-GFP fluorescence in horizontal root caps. Shaded columns: control MS media with traces of DMSO or ethanol to dissolve the different inhibitors used. Indole acetic acid was applied in two different concentrations (1 µM and 50 µM). Abbreviations as in Figure 8. Mean values and *SE* from 23 to 69 samples

of a protein expressed under control of the 35S-CaMV promoter. Whether or not the two other EHB1 homologues in Arabidopsis also participate in this regulation needs to be addressed.

At the moment it is unclear, which cellular processes drive the distribution of EHB1. Thus, chemicals affecting various key pathways were employed to address this topic. First, protein biosynthesis was stalled by applying cycloheximide (Figures 6, 8 and 9). Obviously, blocking protein synthesis completely abolished EHB1 accumulation on the upper side. But, more than this, fading of the EHB1-fluorescence at the bottom was also omitted. We conclude from this observation that accumulation and fading of the signal requires an active component which is missing after blocking protein biosynthesis. Second, brefeldin A was applied. BFA treatment interrupts PIN distribution (Geldner et al., 2001, 2003) by interfering vesicle formation by blocking the ARF-GEF activity of GNOM (Naramoto et al., 2014; Steinmann et al., 1999). Therefore, it is not surprising that EHB1 redistribution was also blocked by BFA. However, BFA has multiple impacts on vesicular traffic. For this reason, it cannot be ruled out that BFA has only an indirect impact on EHB1 distribution, since other subcellular trafficking events might also have an effect on EHB1 traffic. A similar observation could be obtained, if NPA was applied. NPA is well known for its negative impact on auxin-induced bending (Hertel, Lomax, & Briggs, 1983). However, its mode of action is still a matter of a very controversial discussion, recently summarized by Teale and Palme (2018). Despite this NPA is often used to disconnect experimentally auxin transport from its signaling. Taken this into account, it seems likely that BFA and NPA both effect EHB1 distribution by their general impact on vesicle formation, which seemed to be an obligate prerequisite for EHB1 redistribution. All applied drugs also effectively block gravitropic root bending (Figure 9), which does not necessarily mean that root bending is a result of the asymmetrically EHB1 distribution. That bending and EHB1 redistribution do not always essentially match could be observed, if cytochalasin D was applied, intended to rule out symplastic transport of EHB1. Indeed, it could be shown that EHB1 redistribution occurred even in presence of CYD. However, plasmodesmata passage depends on several other processes, which provide a highly flexible system that allows macromolecules quite easy to move from one cell to the other (Nicolas et al., 2017; Sevilem, Yadav, & Helariutta, 2014). This was in line with the observation that root bending was reduced, but not abolished in our experiments and fits with previous findings that CYD has at least in some plant species only a slight but significant effect on root gravitropism, occurring as a result of a reduced gravity perception in statocytes due to disordered cytoskeleton in the statocytes (Staves, Randy, & Carl, 1997).

End-on analysis allowed a quantitative approach to study the kinetics of EHB1 redistribution, as presented in Figures 5 and 7. Interestingly, the time course of EHB1 polarization is roughly correlated but slightly delayed relative to the development of a lateral auxin gradient after a gravitropic stimulus, which was presented in a quite sophisticated approach by Brunoud and co-workers using DII-Venus (Brunoud et al., 2012). Based on these observations, we propose that EHB1 and EHB1 and auxin affect and were affected by each other (see model in Figure 10). From our experimental setup, it could not be ruled out that the time course of native EHB1 quantities sufficient to relay gravitropic signaling occurs much faster under natural conditions, since the high quantity of 35S-CaMV driven EHB1-GFP expression might overload any transport system involved. Thus, it is not clear yet, which effect comes first and which one follows.

It is well established that Ca^{2+}-ions represent important elements of the gravitropic signal transduction chain (Hasenstein & Evans, 1986; Monshausen, Miller, Murphy, & Gilroy, 2011; Plieth & Trewavas, 2002; Shih, DePew, Miller, & Monshausen, 2015). We have previously shown that gravitropic bending is substantially enhanced in loss of function mutants of EHB1, which contains two calcium-binding pockets (Dümmer et al., 2016). A gravitropic stimulation of Arabidopsis seedling elicits Ca^{2+} transients that are characterized by a biphasic Ca^{2+} mobilization (Plieth & Trewavas, 2002). The first signal occurs immediately after the stimulus, the other with a delay of about 2 min. Since EHB1 and AGD12 contain both comparable CaLB binding domains, it is likely that both proteins represent potential targets triggered by this calcium release. Considering this fact and derived from our findings, we have developed a working model for a defined sequence within the network of gravitropic signaling (Figure 10). After root reorientation and subsequent statolith sedimentation movement, a Ca^{2+}-signal derived from an asymmetrically Ca^{2+}-release within the statocytes is triggered, which activates EHB1 and AGD12. Ca^{2+}-bound

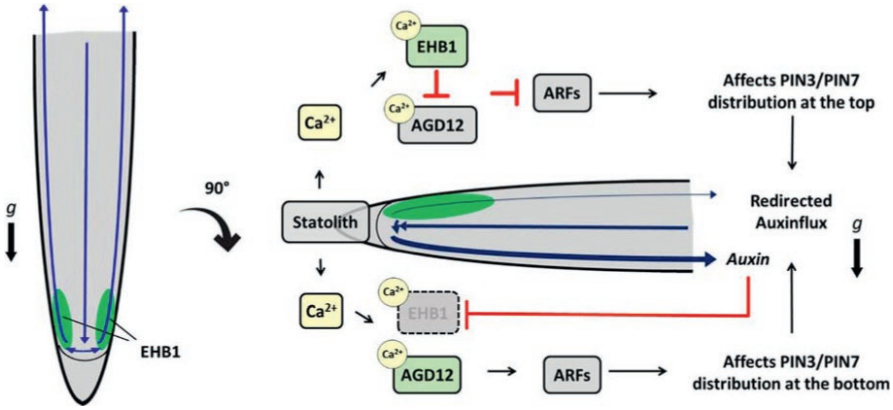

FIGURE 10 Model of early gravitropic signaling involving EHB1 and AGD12 summarizing previous publications and the data presented here. Left: Default situation in vertically growing roots with equally distributed EHB1. Right: After reorientation, statolith movement induces instantaneously an increase of free Ca^{2+}-ions probably by mechanosensitive Ca^{2+}-channels (Plieth & Trewavas, 2002). It is speculated that statholith movement induces an asymmetric top/bottom Ca^{2+}-ratio within the columella (Tatsumi, Toyota, Furuichi, & Sokabe, 2014). Although later gravistimulation also induces a Ca^{2+}-flux from top to bottom (Bjorkman & Cleland, 1991; Lee, Mulkey, & Evans, 1983) and interference with EHB1/AGD12 cannot be ruled out, we propose that EHB1 and AGD12 are triggered by the very initial calcium release. In both cases, EHB1/AGD12 are differentially affected above and below the statocytes. Interference of now calcium-activated EHB1 with either AGD12 or alternatively with its target ARF protein affects ARF-mediated vesicle formation at the top and bottom of the root differently providing an information gradient for a cellular PIN3/7-redistribution, which initiates the redirection of the auxin flux toward the bottom of the root. Downward directed auxin leads to a reduced amount of EHB1 and initiates a further Ca^{2+} release, which subsequently affects cell elongation (Monshausen et al., 2011; Shih et al., 2015). Since EHB1 is degraded at the bottom, an auxin-induced Ca^{2+}-release will have no impact on EHB1 activity

EHB1 gets attached to the membrane comparable to the inhibitory function of EHB1 recently described for iron uptake (Khan et al., 2019) and either affects or competes with AGD12 for ARF-binding. Activated EHB1 can either directly affect/inhibit AGD12 or competes with the protein for ARF binding. Thus, at a very early stage after gravitropic stimulation an information gradient would be generated above and below the statocyte zone, which would cause different ARF-mediated vesicle formation in cells in the upper side compared with the lower side of the root. This could lead to a different PIN3/PIN7 distribution in the affected cells, which would divert the auxin flux. Auxin itself induces a subsequent Ca^{2+}-signal by triggering CNGC14 (Shih et al., 2015), ultimately leading to an asymmetrically cell elongation as proposed by the authors, which would fit quite nicely previous suggestions that calcium regulates auxin and auxin regulates calcium (Vanneste & Friml, 2009). However, if our model is valid, the question has to be addressed whether and how auxin itself affects EHB1 polarization.

Deduced from the auxin-induced reduction of EHB1 presented in Figure 8i,j, we propose the idea that EHB1 might get degraded by an auxin-controlled feedback circuit. This would make sense, since elimination of active EHB1 is necessary during bending, because auxin itself induces Ca^{2+} mobilization at the lower side of the root. In return, this process could induce an EHB1 dependent upward directed counter-movement. At a later stage, after bending is completed, active EHB1 may be important as a prerequisite for the reintroduction of straight vertical growth. However, as mentioned in the result part, this observation needs to be further addressed in more detail. In this context, it would be valuable to know, if and how other Ca^{2+}-ion elements involved in gravitropic signaling, like SYT1 and ROSY1 (Dalal et al., 2016) were linked to this process.

5 | CONCLUSION

Our findings revealed that after a gravitropic stimulation of the root the cellular ratio between EHB1 and AGD12 is affected differently in the upper and lower part of the root tip. This event might provide as a signaling event that ultimately affects the redirection of the lateral auxin flux toward the lower site of the root.

ACKNOWLEDGMENT

We are greatly indebted to Sigrid Völk and Agnes Damm for excellent technical assistance and to the group of Thomas Schmülling (FU Berlin, Germany) for providing seeds of an Arabidopsis GFP-overexpressing line.

CONFLICT OF INTEREST

The authors declare no conflict of interest associated with the work described in this article.

AUTHOR CONTRIBUTIONS

C.F. and P.G. conceived the research design and supervised the experiments, M.R. and M.D. performed the experiments and analyzed the data, C.F. conceived the project and wrote the article with contribution of all the authors.

REFERENCES

Adamowski, M., & Friml, J. (2015). PIN-dependent auxin transport: Action, regulation, and evolution. *The Plant Cell*, *27*, 20–32.

Bjorkman, T., & Cleland, R. E. (1991). The role of extracellular free-calcium gradients in gravitropic signaling in maize roots. *Planta*, *185*, 379–384.

Blakeslee, J. J., Bandyopadhyay, A., Lee, O. R., Mravec, J., Titapiwatanakun, B., Sauer, M., … Murphy, A. S. (2007). Interactions among PIN-FORMED and P-Glycoprotein Auxin Transporters in Arabidopsis. *The Plant Cell*, *19*, 131–147.

Brunoud, G., Wells, D. M., Oliva, M., Larrieu, A., Mirabet, V., Burrow, A. H., … Vernoux, T. (2012). A novel sensor to map auxin response and distribution at high spatio-temporal resolution. *Nature*, *482*, 103.

Clough, S. J., & Bent, A. F. (1998). Floral dip: A simplified method for Agrobacterium-mediated transformation of Arabidopsis thaliana. *The Plant Journal*, *16*, 735–743.

Dalal, J., Lewis, D. R., Tietz, O., Brown, E. M., Brown, C. S., Palme, K., … Sederoff, H. W. (2016). ROSY1, a novel regulator of gravitropic response is a stigmasterol binding protein. *Journal of Plant Physiology*, *196–197*, 28–40.

Dümmer, M., Michalski, C., Essen, L.-O., Rath, M., Galland, P., & Forreiter, C. (2016). EHB1 and AGD12, two calcium-dependent proteins affect gravitropism antagonistically in Arabidopsis thaliana. *Journal of Plant Physiology*, *206*, 114–124.

Geisler, M., Blakeslee, J. J., Bouchard, R., Lee, O. R., Vincenzetti, V., Bandyopadhyay, A., … Martinoia, E. (2005). Cellular efflux of auxin catalyzed by the Arabidopsis MDR/PGP transporter AtPGP1. *The Plant Journal*, *44*, 179–194.

Geldner, N., Anders, N., Wolters, H., Keicher, J., Kornberger, W., Muller, P., … Jurgens, G. (2003). The Arabidopsis GNOM ARF-GEF mediates endosomal recycling, auxin transport, and auxin-dependent plant growth. *Cell*, *112*, 219–230.

Geldner, N., Friml, J., Stierhof, Y. D., Jurgens, G., & Palme, K. (2001). Auxin transport inhibitors block PIN1 cycling and vesicle trafficking. *Nature*, *413*, 425–428.

Hasenstein, K.-H., & Evans, M. L. (1986). Calcium dependence of rapid auxin action in maize roots. *Plant Physiology*, *81*, 439–443.

Hertel, R., Lomax, T. L., & Briggs, W. R. (1983). Auxin transport in membrane vesicles from Cucurbita pepo L. *Planta*, *157*, 193–201.

Hwang, I., & Robinson, D. G. (2009). Transport vesicle formation in plant cells. *Current Opinion in Plant Biology*, *12*, 660–669.

Jensen, R. B., Lykke-Andersen, K., Frandsen, G. I., Nielsen, H. B., Haseloff, J., Jespersen, H. M., … Skriver, K. (2000). Promiscuous and specific phospholipid binding by domains in ZAC, a membrane-associated Arabidopsis protein with an ARF GAP zinc finger and a C2 domain. *Plant Molecular Biology*, *44*, 799–814.

Karimi, M., Inze, D., & Depicker, A. (2002). GATEWAY vectors for Agrobacterium-mediated plant transformation. *Trends in Plant Science*, *7*, 193–195.

Khan, I., Gratz, R., Denezhkin, P., Schott-Verdugo, S. N., Angrand, K., Genders, L., … Ivanov, R. (2019). Calcium-promoted interaction between the C2-domain protein EHB1 and metal transporter IRT1 inhibits Arabidopsis iron acquisition. *Plant Physiology*, *180*(3), 1564–1581.

Kleine-Vehn, J., Leitner, J., Zwiewka, M., Sauer, M., Abas, L., Luschnig, C., & Friml, J. (2008). Differential degradation of PIN2 auxin efflux carrier by retromer-dependent vacuolar targeting. *Proceedings of the National Academy of Sciences of United States of the America*, *105*, 17812–17817.

Knauer, T., Dummer, M., Landgraf, F., & Forreiter, C. (2011). A negative effector of blue light-induced and gravitropic bending in Arabidopsis. *Plant Physiology*, *156*, 439–447.

Lee, J. S., Mulkey, T. J., & Evans, M. L. (1983). Gravity induced polar transport of calcium across root tips of maize. *Plant Physiology*, *73*, 874–876.

Michalski, C., Dümmer, M., Galland, P., & Forreiter, C. (2017). Impact of EHB1 and AGD12 on root and hypocotyl phototropism in Arabidopsis thaliana. *Journal of Plant Growth Regulation*, *36*, 660–668.

Monshausen, G. B., Miller, N. D., Murphy, A. S., & Gilroy, S. (2011). Dynamics of auxin-dependent Ca^{2+} and pH signaling in root growth revealed by integrating high resolution imaging with automated computer vision-based analysis. *The Plant Journal*, *65*, 309–318.

Nalefski, E. A., Wisner, M. A., Chen, J. Z., Sprang, S. R., Fukuda, M., Mikoshiba, K., & Falke, J. J. (2001). C2 domains from different Ca2+ signaling pathways display functional and mechanistic diversity. *Biochemistry*, *40*, 3089–3100.

Naramoto, S. (2017). Polar transport in plants mediated by membrane transporters: Focus on mechanisms of polar auxin transport. *Current Opinion in Plant Biology*, *40*, 8–14.

Naramoto, S., Otegui, M. S., Kutsuna, N., de Rycke, R., Dainobu, T., Karampelias, M., … Friml, J. et al (2014). Insights into the localization and function of the membrane trafficking regulator GNOM ARF-GEF at the Golgi apparatus in Arabidopsis. *The Plant Cell*, *26*, 3062–3076.

Nicolas, W. J., Grison, M. S., Trépout, S., Gaston, A., Fouché, M., Cordelières, F. P., … Bayer, E. M. (2017). Architecture and permeability of post-cytokinesis plasmodesmata lacking cytoplasmic sleeves. *Nature Plants*, *3*, 17082.

Pelham, H. R. B. (1991). Multiple targets for brefeldin A. *Cell*, *67*, 449–451.

Petrasek, J., & Friml, J. (2009). Auxin transport routes in plant development. *Development*, *136*, 2675–2688.

Plieth, C., & Trewavas, A. J. (2002). Reorientation of seedlings in the earth's gravitational field induces cytosolic calcium transients. *Plant Physiology*, *129*, 786–796.

Richter, S., Anders, N., Wolters, H., Beckmann, H., Thomann, A., Heinrich, R., … Jürgens, G. (2010). Role of the GNOM gene in Arabidopsis apical-basal patterning–From mutant phenotype to cellular mechanism of protein action. *European Journal of Cell Biology*, *89*, 138–144.

Robinson, D. G., Hawes, C., Hillmer, S., Jürgens, G., Schwechheimer, C., Stierhof, Y.-D., & Viotti, C. (2018). Auxin and vesicle traffic. *Plant Physiology*, *176*, 1884.

Sevilem, I., Yadav, S. R., & Helariutta, Y. (2014). Plasmodesmata channels for intercellular signaling during plant growth and development. *Methods in Molecular Biology*, *1217*, 3–24

Shih, H. W., DePew, C. L., Miller, N. D., & Monshausen, G. B. (2015). The cyclic nucleotide-gated channel CNGC14 regulates root gravitropism in Arabidopsis thaliana. *Current Biology*, *25*, 3119–3125.

Sot, B., Behrmann, E., Raunser, S., & Wittinghofer, A. (2013). Ras GTPase activating (RasGAP) activity of the dual specificity GAP protein Rasal requires colocalization and C2 domain binding to lipid membranes. *Proceedings of the National Academy of Sciences of the United States of America*, *110*, 111–116.

Staves, M. P., Randy, W., & Carl, L. A. (1997). Cytochalasin D does not inhibit gravitropism in roots. *American Journal of Botany*, *84*, 1530–1535.

Steinmann, T., Geldner, N., Grebe, M., Mangold, S., Jackson, C. L., Paris, S., … Jurgens, G. (1999). Coordinated polar localization of auxin efflux carrier PIN1 by GNOM ARF GEF. *Science*, *286*, 316–318.

Tatsumi, H., Toyota, M., Furuichi, T., & Sokabe, M. (2014). Calcium mobilizations in response to changes in the gravity vector in Arabidopsis seedlings. *Plant Signaling and Behavior*, *9*, e29099.

Teale, W., & Palme, K. (2018). Naphthylphthalamic acid and the mechanism of polar auxin transport. *Journal of Experimental Botany*, *69*, 303–312.

Vanneste, S., & Friml, J. (2009). Auxin: A trigger for change in plant development. *Cell*, *136*, 1005–1016.

Vernoud, V., Horton, A. C., Yang, Z., & Nielsen, E. (2003). Analysis of the small GTPase gene superfamily of Arabidopsis. *Plant Physiology*, *131*, 1191–1208.

Werner, T., Motyka, V., Laucou, V., Smets, R., Van Onckelen, H., & Schmulling, T. (2003). Cytokinin-deficient transgenic Arabidopsis

plants show multiple developmental alterations indicating opposite functions of cytokinins in the regulation of shoot and root meristem activity. *The Plant Cell*, *15*, 2532–2550.

SUPPORTING INFORMATION

Additional supporting information may be found online in the Supporting Information section.

How to cite this article: Rath M, Dümmer M, Galland P, Forreiter C. A gravitropic stimulus alters the distribution of EHB1, a negative effector of root gravitropism in Arabidopsis. *Plant Direct*. 2020;4:1–14. https://doi.org/10.1002/pld3.215